

Lateral instability in streamers discharges

M. Arrayás

*Área de Electromagnetismo, Universidad Rey Juan Carlos,
Camino del Molino s/n, 28943 Fuenlabrada, Madrid, Spain.*

M. A. Fontelos

Instituto de Ciencias Matemáticas, (ICMAT, CSIC-UAM-UCM-UC3M), Campus de Cantoblanco, 28006 Madrid, Spain.

(Dated: January 15, 2022)

In this paper we study the lateral instability of streamer discharges using a continuum discharge model. We observe similarities to Kelvin-Helmholtz instability in fluids. In strong electric fields, lateral long wave length perturbations can grow while small wave length perturbations diminish during the discharge evolution. We perform numerical simulations and carry out asymptotic analysis of the instability. Our results could explain the growth observed in experimental discharges.

Electric discharges pose interesting questions from both applied and fundamental research. They appear in a vast variety of phenomena, ranging from dielectric breakdown in low temperature plasmas and semiconductors [1–3] to high energetic atmosphere activity [4, 5]. During the last twenty years, progress has been made in the understanding of different aspects of the phenomena, such as pattern formation [6]. The study of the branching of the ionization fronts [7–10] has been an example of the progress made. Yet many open questions remain unsolved. One of them is to understand the mechanism by which a streamer in air tends to bend and twist instead of following a straight line. In Fig. 1 we can see the situation appearing in a Tesla coil discharge serving as illustrative purpose of the problem that we address in this work.

We aim to study the transversal wave motion observed in the filaments of electric discharges. As it can be observed in the photograph shown in Fig. 1, there is a transversal modulation in the shape of the filaments produced between the electrodes. The long wave length pattern is found in many different experimental situations in electric discharges and resembles a kind of Kelvin-Helmholtz instability. Our results yield an instability for long wave modes at an interface which is moving under strong field conditions at constant velocity. In this sense, it is similar to the situation arising in other context such as the development of liquid filaments at the interface of two parallel fluid flows due to Kelvin-Helmholtz instability, leading to sprouting of filamentary structures [11]. Here we present the first numerical and analytical evidence pointing in that direction.

We will take a simpler model similar to the standard minimal one which was successfully used in the study of branching [6–8]. Ionization will be the only process taken into account for the generation of charge. However we will add a saturation constraint due to the fact that the ionized channel is depleted of neutral particles so ionization is not allowed inside the plasma.

The balance equations for the electron, positive and

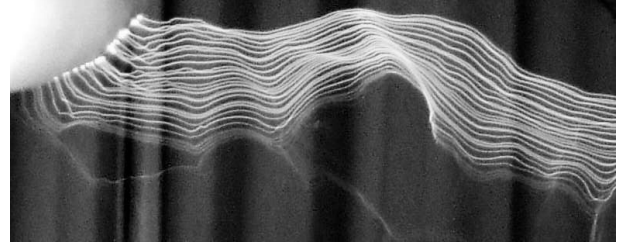


FIG. 1. Electric discharge showing the ribbon-like filaments from a Tesla coil by I. Tresman under Creative Commons license (CC) [12]. We take it merely as illustrative purposes. The lateral or transversal instabilities can be observed in the filaments.

neutral densities, $N_{e,p}$ and N , will be written as

$$\frac{\partial N_e}{\partial \tau} + \nabla_{\mathbf{R}} \cdot \mathbf{J}_e = S_e, \quad (1)$$

$$\frac{\partial N_p}{\partial \tau} = S_p, \quad (2)$$

$$\frac{\partial N}{\partial \tau} = S. \quad (3)$$

At small time-scales the positive ion current can be neglected as it is more than two orders of magnitude smaller than the electron one. If the neutral gas is not moving on average, there will be no net current for N either. The electron current can be written as $\mathbf{J}_e(\mathbf{R}, \tau) = -\mu_e \mathcal{E} N_e - D_e \nabla_{\mathbf{R}} N_e$, where \mathcal{E} is the electric field and μ_e and D_e are the mobility and diffusion coefficients of the electrons. The electric field evolution is governed by the Poisson equation,

$$\nabla_{\mathbf{R}} \cdot \mathcal{E} = \frac{e}{\varepsilon} (N_p - N_e), \quad (4)$$

where ε is the permittivity of the gas and the absolute value of the charge of positive ions is the electron charge e (if it is not the case a Z number has to be introduced which can be removed with an appropriated scaling of the variables).

Now let us introduce the constrain on the production of the charged particles. We will assume that initially we

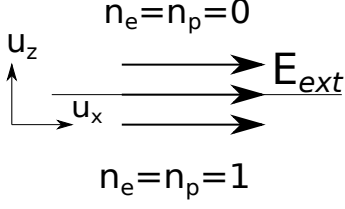


FIG. 2. A schematic of the case considered, where a planar interface parallel to the external field separates two ionized and non-ionized regions.

have a neutral gas of density N_0 , so at any time we will have

$$N_0 = N_p + N, \quad (5)$$

and from that follows, that the source terms $S_p = -S$. On the other hand, due to charge conservation $S_e = S_p$, which relates all the source terms. Considering the production of charge by ionization in Townsend's approximation [9] we get $S_e = N_e \mu_e |\mathcal{E}| N \sigma \exp(-\mathcal{E}_i/|\mathcal{E}|)$.

The densities can be scaled by the initial neutral gas density, thus $n_e = N_e/N_0$, $n_p = N_p/N_0$. The scattering cross section of the ionization process sets a characteristic length $R_0 = 1/N_0\sigma$, and the collision time $\tau_0 = \varepsilon/eN_0\mu_e$ a time scale. Introducing the dimensionless coordinates $\mathbf{r} = \mathbf{R}/R_0$, $t = \tau/\tau_0$, the dimensionless electric field $\mathbf{E} = \mathcal{E}\varepsilon\sigma/e$, and the dimensionless diffusion constant $D = D_e N_0 \sigma^2 \varepsilon / e \mu_e$, the model reads

$$\begin{aligned} \frac{\partial n_e}{\partial t} &= \nabla \cdot (n_e \mathbf{E} + D_e \nabla n_e) + n_e(1 - n_p) |\mathbf{E}| e^{-\alpha/|\mathbf{E}|}, \\ \frac{\partial n_p}{\partial t} &= n_e(1 - n_p) |\mathbf{E}| e^{-\alpha/|\mathbf{E}|}, \\ \nabla \cdot \mathbf{E} &= n_p - n_e. \end{aligned} \quad (6)$$

where $\alpha = \mathcal{E}_i \varepsilon \sigma / e$ is a dimensionless parameter.

Close enough to the discharge channel we will assume that the interface can be approximated by a plane, so we will study the case of a expanding channel with a planar symmetry. We will take Cartesian coordinates on the interface along the x -axis and z -axis, and a constant external field parallel to the interface, given by $\mathbf{E}_{ext} = E_{x0} \mathbf{u}_x$ where $E_{x0} > 0$ and \mathbf{u}_x is a unitary vector in the x direction, as schematically depicted in the Fig. 2. We need to provide the boundary conditions for the system (6) according to the situation considered. Asymptotically at $z \rightarrow -\infty$ we have the discharge channel fully ionized, so $n_e = n_p = 1$ and the electric field will be the external one $\mathbf{E} = E_{x0} \mathbf{u}_x$. At $z \rightarrow +\infty$ the system is neutral and there is not charge, so $n_e = n_p = 0$.

The simulations presented in Fig. 3-4 has been realized in a bigger box of 2×2 dimensionless units using a finite element method. The boundary conditions for the densities are periodic in the x -direction and of Dirichlet type in the z -direction. For the Poisson equation, zero flux is

taken at the z boundaries, i.e. $\mathbf{u}_z \cdot \mathbf{E} = 0$ and we fix the electric potential at the x boundaries so there is an external electric field of $E_{x0} = 1$ intensity in dimensionless units. For the initial conditions we have assumed that the interface is situated at $z = 0$, with $z < 0$ representing the ionized channel filled with $n_e = n_p = 1$ and $z > 0$ the non-ionized region with $n_e = n_p = 0$. In the numerical simulations the parameters appearing in the system (6) are taken as $\alpha = 1$ and $D = 0.02$ for the diffusion coefficient.

In order to study the stability of the channel, we introduce a geometrical perturbation of the interface adding a sinusoidal displacement to the densities distributions around $z = 0$ and then following the evolution. In the figures we plot the electron densities at different times 0.1, 0.3, 0.7. As expected we observe that the perturbation moves to the left, driven by the electric field. At the same time the ionized region expands, and the channel increases the size in the z -direction. In Fig. 3 we have introduced a small wave length perturbation of 0.25 in dimensionless unit. We observe that the perturbation diminishes and eventually disappears. However, larger wave length perturbations will increase as shown in Fig. 4 where the wave length perturbation is 1.

Having presented numerical evidence, let us give some analytical calculations for the onset of the instability observed. We expand the densities and the electric field in a small ϵ parameter in the following form

$$\begin{aligned} n_e &= \phi_e(\xi) + \epsilon n_e^{(1)}(x, z, t) + O(\epsilon^2), \\ n_p &= \phi_p(\xi) + \epsilon n_p^{(1)}(x, z, t) + O(\epsilon^2), \\ \mathbf{E} &= E_x^{(0)} \mathbf{e}_x + \sqrt{D} E_z^{(0)}(\xi) \mathbf{e}_z + \epsilon \mathbf{E}^{(1)}(x, z, t) + O(\epsilon^2). \end{aligned} \quad (7)$$

where

$$\xi = \frac{z - \epsilon f(x, t)}{\sqrt{D}} - ct.$$

Zero order terms represent travelling waves solutions and the function $f(x, t)$ represents the geometrical perturbation of such solutions. Together with the first order terms allow the asymptotic analysis of the instability.

To keep amenable the mathematical analysis and highlight the physical results, we will restrict it to the condition that $|\mathbf{E}| e^{-\alpha/|\mathbf{E}|} \approx 1$, which is a sensible choice provided that $|\mathbf{E}| \approx E_{x0} = 1$, i.e. we have a strong external electric field, and the ionization critical field is lower than this external field, which allows to take the $\alpha \rightarrow 0$ limit. Inserting the expansion (7) in (6) and after some standard but cumbersome algebraic manipulations, we summarize the main results.

To zero order, there are travelling waves solutions which decay at $\xi \rightarrow -\infty$ as

$$\phi_e = 1 - A_1 e^{\alpha_1 \xi} - A_3 e^{\beta_1 \xi} \quad (8)$$

$$\phi_p = 1 - B_1 e^{\beta_1 \xi}, \quad (9)$$

$$E_z^{(0)} = E_3 e^{\alpha_1 \xi} + E_1 e^{\beta_1 \xi}, \quad (10)$$

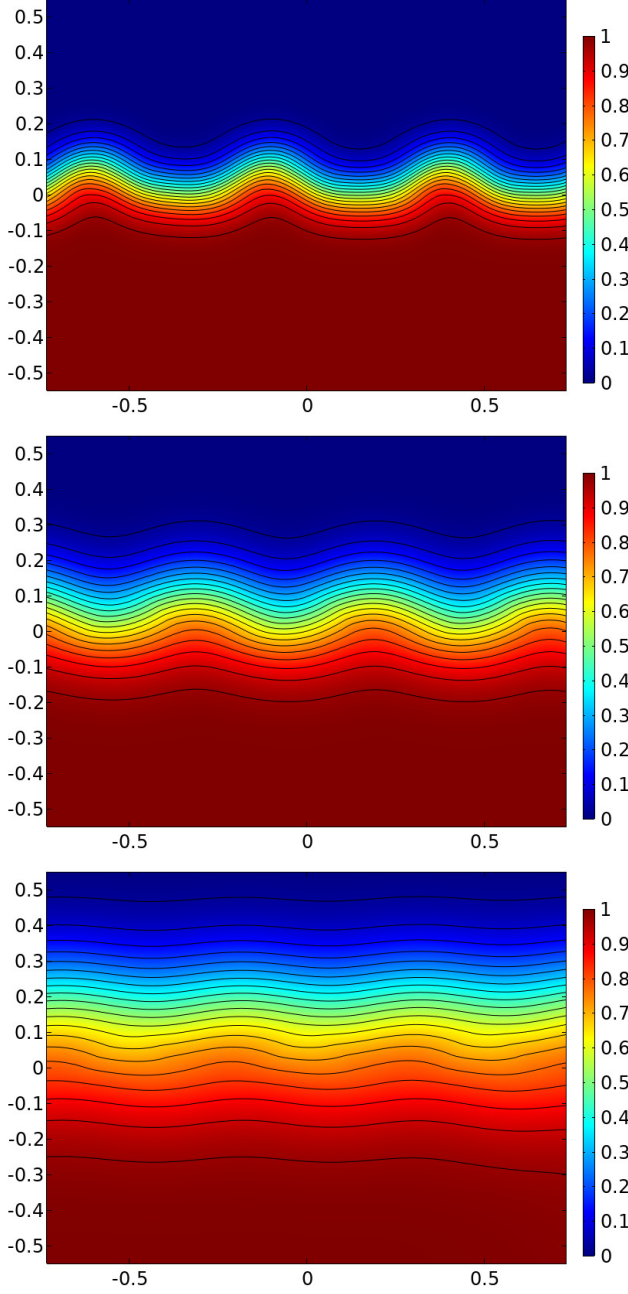


FIG. 3. Electronic density levels evolution at times 0.1, 0.3 and 0.7 from top to bottom. The initial perturbation of the electronic density moves towards left, drifted by the electric field while decreases its amplitude.

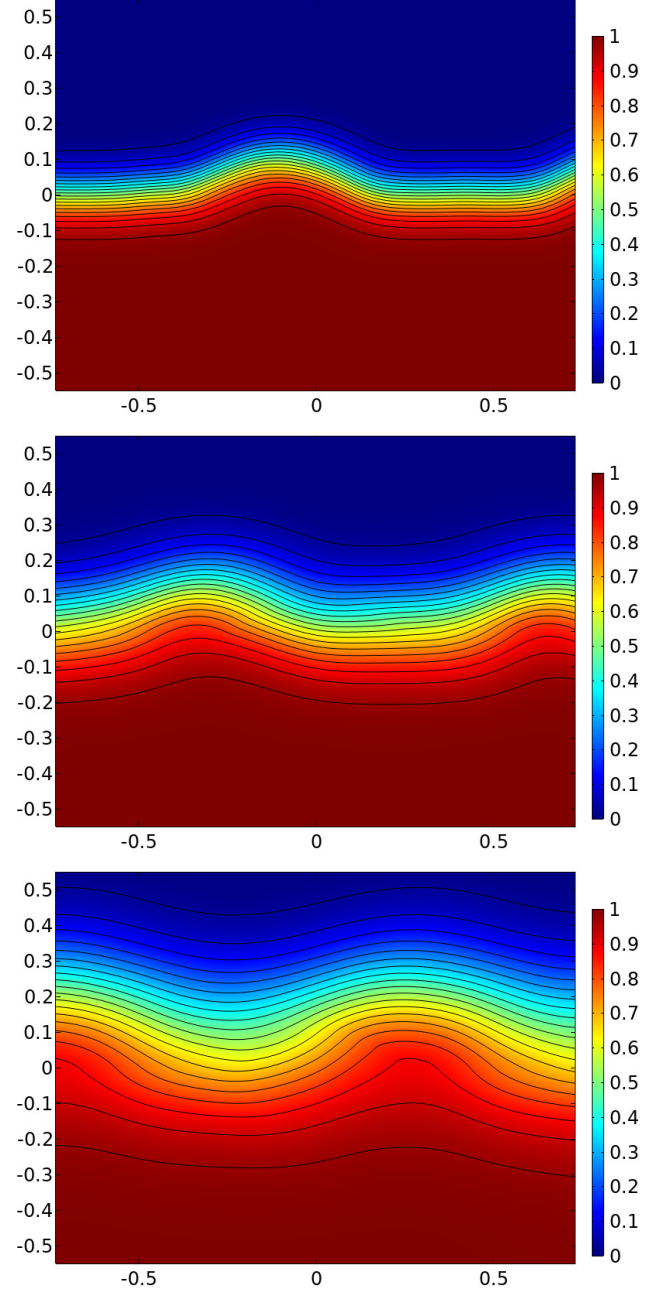


FIG. 4. Electronic density levels evolution at times 0.1, 0.3 and 0.7 from top to bottom. The initial perturbation of the electronic density moves towards left, drifted by the electric field but the amplitude increases.

for $\xi \rightarrow +\infty$ is

$$\phi_e = A_2 e^{-\beta_2 \xi}, \quad (11)$$

$$\phi_p = B_2 e^{-\beta_2 \xi}, \quad (12)$$

$$E_z^{(0)} = E_0 + E_2 e^{-\beta_2 \xi}, \quad (13)$$

where A_1, A_3, B_1, E_1 and E_3 are constants determined by the boundary conditions and $\alpha_1 > \beta_1$ the corresponding positive eigenvalues that can be written in terms of the wave velocity c . The behaviour of such travelling waves

where again A_2, B_2, E_0 and E_2 are constants and $\beta_2 > 0$ the corresponding eigenvalue that can be expressed as a function of c . A standard shooting technique allows then

to determine the appropriate value of c so that the exponential decays in (8)-(13) are satisfied. Notice that to zero order, if E_0 is non vanishing, there is an electric field at infinity in the z -direction due to the contribution of the travelling wave unbalanced charged. Indeed considering the limit $D \rightarrow 0$ it can be shown that the travelling wave propagating speed c reaches an extremum if $E_0 = 0$, and in this case, $c \approx 2.0$.

The travelling wave solution for $E_0 = 0$ is such that the profile for negative charges is, due to their larger mobility, slightly ahead/behind the profile for positive charges as z approaches plus/minus infinity. This leads to a profile for the net charge that changes sign at the interface and decays fast at infinity. Thus, charges behave effectively as dipoles concentrated at the interface in a region of $O(\sqrt{D})$ thickness. Nevertheless, the fact that negative charges are mobile (due to drift by the electric field and diffusion) while the positive charges are not indicates that such dipolar configuration cannot remain stable when the interface is not flat. This fact will be visible at the next order.

To first order contribution, the geometric shape function $f(x, t)$ is governed by

$$-f_t + f_x - E_z^{(1)}|_{\xi=0} + Df_{xx} = 0, \quad (14)$$

in which appears the z component of the electric field perturbation evaluated at $\xi = 0$. When the geometrical evolution follows (14), the equation for the evolution of $n_e^{(1)}$ turns out to be a homogeneous one, so we can choose $n_e^{(1)} = 0$. Electrons are mobile and may follow a geometrical perturbation without changes in their density. However, this is not the case for $n_p^{(1)}$ since positive charges cannot follow the electric field. Hence, a deficit in positive charges appears in the computation of the electric field in (14).

The physical argument is that the positive charge do not move, so the perturbation of the electron density implies the appearance of an extra charge in addition to the created by the travelling wave. Writing $f(x, t) = F(x)e^{\lambda t}$, the asymptotic behaviour $n_p^{(1)} = N_p^{(1)}e^{\lambda t}F(x)$ is then found as

$$N_p^{(1)} \sim \begin{cases} N_1^- e^{\mu_1 \xi}, & \text{as } \xi \rightarrow -\infty, \\ N_1^+ e^{-\mu_2 \xi}, & \text{as } \xi \rightarrow +\infty \end{cases} \quad (15)$$

with

$$N_1^- = B_1 \mu_1 / \sqrt{D}, \quad N_1^+ = \frac{\lambda B_2 \mu_2}{\lambda \sqrt{D} + c \mu_2 \sqrt{D}} \quad (16)$$

Introducing an electric potential, at first order in ϵ we get the equation

$$-\Delta V^{(1)} = -\sqrt{D} f_{xx} E_z^0 + n_p^{(1)}, \quad (17)$$

and then $E_z^{(1)} = -\partial V^{(1)} / \partial z$ at $\xi = 0$ has to be inserted into (14) for the evolution of f . The solution turns out

to be

$$E_z^{(1)} = -\sqrt{D} k^2 F(\sqrt{D} k) - G_1(\sqrt{D} k) + \frac{\lambda}{\sqrt{D} \lambda + \sqrt{D} c \mu_2} G_2(\sqrt{D} k), \quad (18)$$

where

$$F(s) = \frac{1}{2\pi} \int_{-\infty}^{\infty} \frac{(\nu^2(E_2 - E_1) + \beta_1^2 E_2 - \beta_2^2 E_1)}{(s^2 + \nu^2)(\nu^2 + \beta_1^2)(\nu^2 + \beta_2^2)} \nu^2 d\nu, \quad (19)$$

and

$$G_{1,2}(s) = \frac{1}{2\pi} \int_{-\infty}^{\infty} \frac{B_{1,2} \mu_{1,2}}{(s^2 + \nu^2)(\nu^2 + \mu_{1,2}^2)} \nu^2 d\nu. \quad (20)$$

We can now use (14) to deduce the dispersion relation

$$-\lambda + ik - Dk^2 + Dk^2 F(\sqrt{D} k) + G_1(\sqrt{D} k) - \frac{\lambda}{\sqrt{D}(\lambda + c \mu_2)} G_2(\sqrt{D} k) = 0. \quad (21)$$

In the limit D small we can approximate it as

$$\lambda \left(1 + \frac{G_2(\sqrt{D} k)}{\sqrt{D} c \mu_2} \right) \approx ik - Dk^2 + Dk^2 F(\sqrt{D} k) + G_1(\sqrt{D} k).$$

The onset on the instability starts when $Re(\lambda) \rightarrow 0$, which in terms of $s_c = \sqrt{D} k_c$ implies

$$G_1(s_c) = s_c^2 (1 - F(s_c)) \quad (22)$$

Numerically one can compute travelling waves solutions and get the values $\beta_1 \simeq 0.37$, $E_1 \simeq 0.67$, $\beta_2 \simeq 0.8$, $E_2 \simeq 2.71$, $\mu_1 \simeq 0.5$, $B_1 \simeq 0.4$, $\mu_2 \simeq 0.9$, $B_2 \simeq 7.4$. Using the definitions (19) and (20) it can be numerically estimated the value of s_c as $s_c \simeq 0.5$ and hence instabilities may take place for

$$\sqrt{D} \frac{2\pi}{\lambda} \lesssim 0.5 \quad (23)$$

implying $\lambda \gtrsim 12.6\sqrt{D}$, i.e. long wave length instabilities as observed in the simulations.

In this article we have studied the problem of the lateral pattern observed in electric discharges. A plasma filament tends to bend and twist as the discharge progresses. Using a simplified model we have found evidence of the onset of long wave instabilities, similar to the Kelvin-Helmholtz type in fluid dynamics. The evidence of the growth of long wave perturbations has been obtained both numerically and theoretically, by solving the model using finite difference methods and by asymptotic analysis of the particular case of a planar interface.

M. Arrayás and M.A. Fontelos are supported by the research Grants from the Spanish Ministry of Economy and Competitiveness, ESP2017-86263-C4-3-R and MTM2017-89423-P respectively.

-
- [1] A. Kolobov, Phys. Plasmas **20**, 101610 (2013).
 - [2] A. S. Kyuregyan, Phys. Rev. E **89**, 042916 (2014).
 - [3] A. Luque, M. González, and F. J. Gordillo-Vázquez, Plasma Sources Sci. Technol. **5**, 117 (1996). **26**, 125006 (2017).
 - [4] A. Luque and F. J. Gordillo-Vázquez, Nature Geoscience **5**, 22 (2011).
 - [5] O. A. van der Velde, J. Montanyà, J. A. López, and S. A. Cummer, Nature Comm. **10**, 4350 (2019).
 - [6] U. Ebert, W. van Saarloos, and C. Caroli, Phys. Rev. Lett. **77**, 4178 (1996).
 - [7] M. Arrayás, U. Ebert, and W. Hundsdorfer, Phys. Rev. Lett. **88**, 174502 (2002).
 - [8] M. Arrayás, M. A. Fontelos, and J. L. Trueba, Phys. Rev. Lett. **95**, 165001 (2005).
 - [9] M. Arrayás, S. Betelú, M. A. Fontelos, and J. L. Trueba, SIAM J. Appl. Math. **68**, 1122 (2008).
 - [10] M. Arrayás, M. A. Fontelos, and U. Kindelán, Phys. Rev. E **86**, 066407 (2012).
 - [11] D. Fuster, J. Matas, S. Marty, S. Popinet, J. Hoepffner, A. Cartellier, and S. Zaleski, J. Fluid Mech. **736**, 150 (2013).
 - [12] Photograph taken by Ian Tresman at the UK Teslathon in Derby, UK, on 27 May 2005. The figure has been rotated 90 degrees. The photo is licensed under the Creative Commons Attribution 2.5 Generic, <https://creativecommons.org/licenses/by/2.5/deed.en>.